

1 How does the strength of selection influence genetic
2 correlations ?

3 Stéphane Chantepie^{*,1} and Luis-Miguel Chevin^{*,2}

4 ¹Independent Researcher, Antony, France

5 ²Centre d'Ecologie Fonctionnelle et Evolutive (CEFE), CNRS, University of
6 Montpellier, University of Paul Valéry Montpellier 3, EPHE, IRD, France

7 **Keywords:** stabilizing selection, genetic variance-covariance matrix, genetic drift, selection-
8 mutation-drift equilibrium, genetic correlation

9 **Abstract Word Count:** 199

10 **Total Word Count:** 4833

11 ***Corresponding authors:** schantepie@protonmail.com; luis-miguel.chevin@cefe.cnrs.fr

12

Abstract

13

14

15

16

17

18

19

20

21

22

23

24

25

26

27

28

29

30

Genetic correlations between traits can strongly impact evolutionary responses to selection, and may thus impose constraints on adaptation. Theoretical and empirical work has made it clear that, without strong linkage, genetic correlations at evolutionary equilibrium result from an interplay of correlated pleiotropic effects of mutations, and correlational selection favoring combinations of trait values. However, it is not entirely clear how the strength of stabilizing selection influences this compromise between mutation and selection effects on genetic correlations. Here, we show that the answer to this question crucially depends on the intensity of genetic drift. In large, effectively infinite populations, genetic correlations are unaffected by the strength of selection, regardless of whether the genetic architecture involves common small-effect mutations (Gaussian regime), or rare large-effect mutations (House-of-Cards regime). In contrast in finite populations, the strength of selection does affect genetic correlations, by shifting the balance from drift-dominated to selection-dominated evolutionary dynamics. The transition between these domains depends on mutation parameters to some extent, but with a similar dependence of genetic correlation on the strength of selection. Our results are particularly relevant for understanding how senescence shapes patterns of genetic correlations across ages, and genetic constraints on adaptation during colonization of novel habitats.

31 Introduction

32 Adaptation is inherently a multidimensional problem. Organisms live in complex environ-
33 nments composed of multiple niche axes (Hutchinson, 1957), which exert natural selection
34 on phenotypes composed of multiple traits that get integrated during development (Fisher,
35 1930). This complexity can limit the process of adaptive evolution. First, the mere fact that
36 multiple traits are under selection can slow down adaptation, which has been described as
37 the cost of complexity (Fisher, 1930; Orr, 2000). And second, genetic correlations between
38 traits can constrain the response to selection for any of these traits, thereby limiting the en-
39 suing increase in fitness by adaptive evolution (Hansen and Houle, 2008; Walsh and Blows,
40 2009; Lande, 1979; Chevin, 2013; Agrawal and Stinchcombe, 2009; Connallon and Hall, 2018;
41 Etterson and Shaw, 2001). The evolutionary quantitative genetics theory underlying these
42 predictions (Lande, 1979) was soon followed by a related formalism for measuring selection
43 on correlated characters (Lande and Arnold, 1983; Lande, 1979). This has fostered much
44 interest in the last decades for measuring patterns of genetic correlations among traits, in
45 order to quantify constraints on adaptation (reviewed in Agrawal and Stinchcombe, 2009).
46 Such constraints can also be interpreted geometrically (Walsh and Blows, 2009), as genetic
47 correlations can influence the major axis of genetic variation across multiple traits, orienting
48 evolution along lines of least resistance (Schluter, 1996).

49 Beyond quantifying the consequences of genetic correlations on rates on adaptation, un-
50 derstanding what shapes constraints on adaptation ultimately requires investigating the
51 factors that govern the evolution of the \mathbf{G} matrix, which includes all the additive genetic

52 variances of traits and covariances among traits (Lande, 1979). This has been a topic of
53 intense research, both theoretically and empirically. Theoretical work has made it clear that
54 genetic correlations evolve in response to (i) correlated pleiotropic mutation effects on traits,
55 and (ii) correlational selection favoring combinations of trait values between pairs of traits
56 (Lande, 1980; Turelli, 1985). Random genetic drift may also play an important role (Jones
57 et al., 2003), but this was mostly investigated through individual-based simulations, and few
58 analytical results exist to guide intuition in that respect. In addition, patterns of environ-
59 mental change (Jones et al., 2004, 2012) and epistatic interactions among loci (Jones et al.,
60 2014) can also influence the shape of the \mathbf{G} matrix and evolution of genetic correlation, but
61 we will not address them here. On the empirical side, it was recently demonstrated that
62 the genetic divergence of multiple traits across several *Drosophila* species is aligned with the
63 major axis of both the \mathbf{G} matrix of additive genetic variation within species, and the \mathbf{M}
64 matrix of mutation effects on these traits (Houle et al., 2017). Natural selection was not
65 measured in that study, but another study on the same set of traits has demonstrated that
66 their genetic correlations can evolve in response to experimental patterns of correlational
67 selection (Bolstad et al., 2015).

68 Since genetic correlations result from a compromise between mutational correlations and
69 correlational selection, we may wonder: how do they change as the strength of selection
70 varies? And more generally: how does the overall shape of the \mathbf{G} matrix change as a fitness
71 peak becomes broader (thus causing weaker selection), or narrower (stronger selection),
72 while keeping the same overall shape (as illustrated in Fig. 1a)? This simple question has

73 received surprisingly little attention, despite its general importance in evolutionary biology.
74 In particular, it bears on our understanding of the evolution of senescence by mutation
75 accumulation, whereby relaxed selection on later age classes allow for accumulation of more
76 genetic variance of traits (Charlesworth and Hughes, 1996). A multivariate extension of this
77 argument might suggest that the \mathbf{G} matrix becomes more similar to the mutation \mathbf{M} matrix
78 in older ages, because they undergo relaxed selection. However, the premises that underlie
79 this argument have yet to be explored more thoroughly.

80 Here, we investigate theoretically how the overall strength of selection influences evolution
81 of genetic correlations, and the shape and orientation of the \mathbf{G} matrix. Using analytical
82 results and individual based simulations, we show that the relative importance of mutation
83 vs selection in shaping the \mathbf{G} matrix critically depends on random genetic drift.

84 **Methods**

85 **Model**

86 As in standard quantitative genetic models, we assume that the multivariate phenotype \mathbf{z} can
87 be partitioned into a breeding value determined by the genotype, plus a residual component
88 of variation (often described as the environmental component), which is normally distributed
89 with mean 0 and covariance matrix \mathbf{E} . In each generation, mutations occur with probability μ
90 at each allele of n diploid loci, such that the total mutation rate is $2n\mu$. Mutation increments
91 the phenotypic value at the mutated allele by an effect that is unbiased (does not change the

92 average breeding value), but can change the genetic (co)variances between traits. Specifically,
93 we assume multivariate normally distributed mutation effects $\boldsymbol{\alpha}$, with mean 0 and the same
94 covariance matrix \mathbf{M} at each locus, which we parameterize (for two traits) as

$$\begin{aligned}\mathbf{M} &= V_{\alpha}\mathbf{M}_{\rho} \\ \mathbf{M}_{\rho} &= \begin{pmatrix} 1 & \rho_m\sqrt{\phi_m} \\ \rho_m\sqrt{\phi_m} & \phi_m \end{pmatrix}.\end{aligned}\tag{1}$$

95 The parameter V_{α} is the variance of mutation effects on trait 1 (a scalar), ϕ_m is the ratio
96 of mutational variances between traits 2 and 1, and ρ_m is the mutational correlation. When
97 $\phi_m = 1$ the two traits have the same mutational variance, and \mathbf{M}_{ρ} is a mutational correla-
98 tion matrix. The multivariate phenotype is under stabilizing selection towards an optimum
99 phenotype $\boldsymbol{\theta}$, which we assume constant for simplicity. This is modeled as classically by
100 letting the fitness of individuals with multivariate phenotype \mathbf{z} (relative to the fitness of the
101 optimum phenotype) be

$$W(\mathbf{z}) = \exp\left(-\frac{(\mathbf{z} - \boldsymbol{\theta})^T \boldsymbol{\Omega}^{-1}(\mathbf{z} - \boldsymbol{\theta})}{2}\right)\tag{2}$$

102 where the matrix $\boldsymbol{\Omega}$ determines the breadth and orientation of the fitness peak. Averaging
103 over the distribution of residual phenotypic variation, the fitness function on breeding values
104 \mathbf{x} (relative to the fitness of the optimum breeding value), which determines evolution of the
105 \mathbf{G} matrix, is

$$\tilde{W}(\mathbf{z}) = \exp\left(-\frac{(\mathbf{x} - \boldsymbol{\theta})^T \mathbf{V}^{-1}(\mathbf{x} - \boldsymbol{\theta})}{2}\right)\tag{3}$$

106 where $\mathbf{V} = \boldsymbol{\Omega} + \mathbf{E}$ is the stabilizing selection matrix. Note that because of residual non-
107 heritable phenotypic variation, the absolute fitness of individuals with a given breeding

108 value \mathbf{x} is actually reduced, by a factor $\sqrt{\det(\mathbf{V}^{-1}\mathbf{\Omega})}$ (where \det denotes the determinant
109 of a matrix), relative to that of individuals with the same realized phenotype $\mathbf{z} = \mathbf{x}$. This
110 amounts to reducing the effective number of parents in the population: even in a Wright-
111 Fisher population of size N , the effective size that matters for random genetic drift (change
112 in the distribution of breeding values) is in fact $N_e = \sqrt{\det(\mathbf{V}^{-1}\mathbf{\Omega})}N$ (and in a non-Wright-
113 Fisher population, N should be replaced by the effective size operating at the level of the
114 expressed phenotypic trait). In other words, selection on non-heritable phenotypic variation
115 increases the intensity of genetic drift on heritable phenotypic variation. This fact, which
116 was largely overlooked in previous studies on this topic (e.g. Lande, 1976, 1979; Burger et al.,
117 1989), becomes important under strong selection and low population size.

118 The selection matrix \mathbf{V} can be written similarly to \mathbf{M} as

$$\mathbf{V} = V_s \mathbf{V}_\rho$$
$$\mathbf{V}_\rho = \begin{pmatrix} 1 & \rho_s \sqrt{\phi_s} \\ \rho_s \sqrt{\phi_s} & \phi_s \end{pmatrix}. \quad (4)$$

119 The scalar V_s determines the width of the fitness peak on breeding values, and is inversely
120 proportional to the strength of stabilizing selection, while ϕ_s controls the ratio of strengths
121 of selection between the two traits. The selective correlation ρ_s determines what genetic cor-
122 relation is favored by natural selection. Figure 1a illustrates how these parameters translate
123 into the shapes of the mutation and selection matrix.

124 Individual-based simulations

125 We tested the accuracy of expected \mathbf{G} matrix and genetic correlation at mutation-selection(-
126 drift) equilibrium using individual-based, genetically explicit simulations. The traits were
127 determined by $n = 50$ unlinked diploid loci, with alleles assumed to be fully pleiotropic
128 (i.e. affecting all the phenotypic traits under selection). We simulated populations of
129 hermaphroditic, sexually reproducing individuals with non-overlapping generations. The
130 life cycle included three steps :

- 131 1. **Computing the phenotype and fitness for each individual.** For each trait, the
132 phenotype was estimated by summing breeding values across all loci and alleles. A
133 residual component of variation was then added for each trait, with mean 0, variance
134 1, and no covariance between traits. The expected fitness of each individual was then
135 computed based on their phenotypic values and the stabilizing selection matrix $\mathbf{\Omega}$, as
136 defined by equation (2). The fitness optimum was arbitrarily set to zero.
- 137 2. **Sequential reproduction based on reproductive fitness.** Two adults were drawn
138 randomly with a probability equal to their expected fitness and mated to produce
139 exactly one offspring. Selfing was not allowed, and being involved in a reproductive
140 event did not change the probability to mate again. The sequence was repeated N
141 times.
- 142 3. **Offspring production.** The genotypes of offspring were produced by drawing one
143 random allele from each parent at each locus, thus modelling fully unlinked loci. The
144 probability that a mutation occurred a each allele of each locus was μ . Mutation had

145 additive effect on the traits, modifying the phenotypic value of the mutated allele by
146 an amount drawn from a multivariate normal distribution, with means zero (unbiased
147 mutation) and mutation variance-covariance matrix \mathbf{M} .

148 This life cycle, developed by Revell (2007), ensures that the population size N is constant
149 and equal to the effective population size N_e in the absence of selection. Here, to account for
150 the reduction in effective population size caused by selection on the residual component of
151 variation (see previous section), for each required value of N_e we used $N = N_e / \sqrt{\det(\mathbf{V}^{-1}\mathbf{\Omega})}$
152 as the population size in the simulations. Since all our formulas depended on the matrix \mathbf{V} of
153 selection on breeding values (eq. (3)), rather than the matrix $\mathbf{\Omega}$ for selection on the expressed
154 phenotype (eq. (2)), we parameterized simulations in terms of \mathbf{V} , and then transformed them
155 to $\mathbf{\Omega}$ before starting the simulation using $\mathbf{\Omega} = \mathbf{V} - \mathbf{E}$ (as per eq. (3)), where $\mathbf{E} = \mathbf{I}$ under
156 our assumption of uncorrelated environmental effects with variance 1.

157 Individual-based simulations were all run over 50000 generations. To ensure that the
158 expected genetic covariance matrix $\bar{\mathbf{G}}$ was estimated after a pseudo-equilibrium is reached
159 (i.e., at stationarity), only the 30000 last iterations from the chain were used to estimate the
160 mean.

161 Results

162 Without drift, genetic correlations are unchanged by selection strength

163 Using similar assumptions as here, Zhang and Hill (2003) showed that in an infinite pop-
164 ulation, and in the limit of rare mutations of large effect (so-called House-of-Cards regime,
165 HoC below; Turelli, 1984, 1985; Bulmer, 1989; Bürger, 2000; Johnson and Barton, 2005), the
166 genetic correlation ρ_G between two traits at mutation-selection balance with weakly linked
167 loci is

$$\rho_G = \frac{\rho_s \sqrt{1 - \rho_m^2} + \rho_m \sqrt{1 - \rho_s^2}}{\sqrt{2 - (\rho_m^2 + \rho_s^2) + \sqrt{(1 - \rho_s^2)(1 - \rho_m^2)}(\phi + \frac{1}{\phi})}} \quad (5)$$

168 where $\phi = \sqrt{\frac{\phi_m}{\phi_s}}$. Remarkably, this shows that genetic correlations at mutation-selection
169 balance depend neither on the absolute strength of stabilizing selection V_s^{-1} nor on the mag-
170 nitude of mutational variance V_α , but instead on the ratio of strengths of stabilizing selection
171 between the two traits, times the ratio of their mutation variances (summarized by the com-
172 pound parameter ϕ). This means that narrowing the fitness peak, thereby increasing the
173 strength of stabilizing selection on all traits, does not tilt the balance of genetic correlations
174 ρ_G towards selective correlations ρ_s and away from mutational correlations ρ_m , as long as
175 the overall shape of the mutation and selection matrices do not change. The same is true of
176 increasing the mutational variance and covariances of all traits by the same factor. In the
177 special case where $\phi = 1$, such that the the ratio of strengths of stabilizing selection on the
178 two traits equals the ratio of their mutational variances, equation (5) further simplifies as

$$\rho_{G,\phi=1} = \frac{\rho_s \sqrt{1 - \rho_m^2} + \rho_m \sqrt{1 - \rho_s^2}}{\sqrt{1 - \rho_m^2} + \sqrt{1 - \rho_s^2}} \quad (6)$$

179 which only depends on mutational and selective correlations.

180 This result was obtained under the HoC regime, which is known to have different prop-
181 erties from a regime of common mutations of weak effect, known as the Gaussian regime
182 (Kimura, 1965; Lande, 1976; Bulmer, 1989; Bürger, 2000; Johnson and Barton, 2005). But
183 in fact, genetic correlations also do not depend on the strength of selection under the Gaus-
184 sian regime. To see this, we rewrite the equilibrium for the \mathbf{G} matrix derived by Lande
185 (1980) under the Gaussian regime, replacing \mathbf{V} and \mathbf{M} with their expressions in equations
186 (1) and (4), to get

$$\mathbf{G} = 2n\sqrt{\mu V_\alpha V_s} \mathbf{V}_\rho^{\frac{1}{2}} \left[\mathbf{V}_\rho^{-\frac{1}{2}} \mathbf{M}_\rho \mathbf{V}_\rho^{-\frac{1}{2}} \right]^{\frac{1}{2}} \mathbf{V}_\rho^{\frac{1}{2}}. \quad (7)$$

187 The first scalar term is the same as for the genetic variance of a single trait at mutation-
188 selection balance in this regime (Kimura, 1965; Lande, 1976). The second term is a matrix
189 that captures all the features of \mathbf{G} matrix shape, including genetic correlations. Equation (7)
190 shows that changing the overall strength of selection V_s^{-1} , or the scale of mutational variance
191 V_m , only magnifies or shrinks the \mathbf{G} matrix, but does not change genetic correlations in any
192 way, nor any other aspect of \mathbf{G} matrix shape.

193 Figure 1 shows examples of \mathbf{G} matrices under variable strength of stabilizing selection
194 (where the fitness peak becomes broader, and selection becomes weaker, as V_s increases,
195 Fig. 1a), in the Gaussian regime. Continuous ellipses in Figure 1b represent the analytical
196 prediction for \mathbf{G} from equation (7), while dashed ellipses show results from genetically explicit
197 individual-based simulations (IBM) using the same parameters, but finite population size
198 $N_e = 5000$. The prediction that the strength of stabilizing selection does not affect the

199 orientation of the \mathbf{G} matrix in a infinite population is already close to holding in simulations
200 with $N_e = 5000$. The volume of the \mathbf{G} matrix increases, but its orientation and shape
201 change little as the strength of selection decreases. The resulting genetic correlation is also
202 little influenced by the strength of selection in simulations with $N_e = 5000$ (dark blue dots
203 in Figure 2b), and remains close to the expected compromise between the mutational and
204 selective correlations predicted by equation (5) (black line in Figure 2b), which does not
205 depend on V_s .

206 Even though the Gaussian and Hoc regime have very different properties in terms of the
207 maintenance of genetic variance for each trait (Turelli, 1985; Bürger, 2000), they strikingly
208 lead to the same genetic correlation among traits in an infinite population. This was already
209 suggested in numerical explorations by Turelli (1985), but we confirmed this here more
210 extensively. In particular, when $\phi_m = \phi_s = 1$, such that the mutation and selection matrices
211 are both proportional to correlation matrices (with only 1 on the diagonal), then deriving the
212 genetic correlation in the Gaussian case from the \mathbf{G} matrix in equation (7) leads to equation
213 (6). In the more general case, an analytical formula also exists for the genetic correlation
214 based on equation (7), but it is unwieldy. Instead of comparing Gaussian and Hoc formulas
215 for genetic correlation, we drew random matrices \mathbf{V} and \mathbf{M} from a Wishart distribution
216 (with expectation \mathbf{I}), a natural distribution for covariance matrices, which allows variance
217 and covariance terms to vary randomly. We then computed the expected \mathbf{G} matrix under
218 the Gaussian regime (from eq. (7)), from which we extracted genetic correlations, which
219 we then compared to equation (5). Figure 2a shows that the genetic correlation under the

220 Gaussian regime, which assumes frequent mutations of small effects, is perfectly predicted by
221 that under the House-of-Card regime, which instead assumes rare mutations of large effects.
222 The blue dots in Figure 2c show genetic correlations for different values of the selection
223 parameter V_s , estimated from individual-based simulations with parameters that correspond
224 to the HoC regime. These correlations are very similar to those in the Gaussian regime in
225 Figure 2b, and close to their expectation in eq. (5).

226 In short, genetic correlations at mutation-selection balance do not change with the overall
227 strength of stabilizing selection, and this conclusion holds generally across a broad range of
228 mutation and selection parameters, spanning different evolutionary regimes. So should we
229 then conclude that correlational selection always has the same influence on genetic correla-
230 tions, and never becomes dominated by the influence of mutational correlations, even as the
231 strength of selection becomes vanishingly small?

232 **Drift controls the balance between mutation and selection's effects** 233 **on genetic correlations**

234 In fact, genetic correlations may indeed become more similar to mutational correlations
235 as the strength of selection decreases, but only in the presence of random genetic drift.
236 In a population with finite effective size N_e , random genetic drift causes a reduction in
237 heterozygosity, and thus in additive genetic variance, by a proportion $2N_e$ per generation.
238 Accounting for this effect, we found that the expected \mathbf{G} matrix at mutation-selection-drift
239 equilibrium in the Gaussian regime is (Appendix A1)

$$\overline{\mathbf{G}} = 2n\sqrt{\mu V_\alpha V_s} \mathbf{V}_\rho^{\frac{1}{2}} \left[\left(\kappa \mathbf{I}^2 + \mathbf{V}_\rho^{-\frac{1}{2}} \mathbf{M}_\rho \mathbf{V}_\rho^{-\frac{1}{2}} \right)^{\frac{1}{2}} - \sqrt{\kappa} \mathbf{I} \right] \mathbf{V}_\rho^{\frac{1}{2}} \quad (8)$$

$$\kappa = \frac{V_s}{(4N_e)^2 \mu V_\alpha}$$

240 where $\overline{\mathbf{G}}$ denotes an expectation over the stochastic evolutionary process (because of random
 241 genetic drift). As in equation (7), the first scalar term in equation (8) is the same as for the
 242 genetic variance of a single trait at mutation-selection balance in this regime (Kimura, 1965;
 243 Lande, 1976), while the matrix product determines \mathbf{G} matrix shape. Equation (8) shows that
 244 a single compound scalar parameter, $\kappa = V_s / [(4N_e)^2 \mu V_\alpha]$, determines how the orientation and
 245 shape of the expected \mathbf{G} matrix change under mutation, selection, and drift (since elements
 246 of \mathbf{V}_ρ and \mathbf{M}_ρ scale on the order 1 by construction). When $V_s \ll (4N_e)^2 \mu V_\alpha$ (κ very small),
 247 the mutation rate and mean selection coefficient of new mutations are both large relative to
 248 the intensity of drift (proportional to $1/N_e$), so genetic correlations are mostly determined
 249 by mutation and selection, with little influence of genetic drift. In the limit $\kappa \rightarrow 0$, equation
 250 (8) tends to the mutation-selection balance in equation (7). In contrast, drift dominates
 251 when $V_s \gg (4N_e)^2 \mu V_\alpha$ (κ very large), and the expected \mathbf{G} matrix then becomes increasingly
 252 similar to the mutation matrix \mathbf{M} . This can be seen when comparing \mathbf{G} matrices in panels
 253 b to e in Figure 1, as well as genetic correlations for different darknesses of blue in Figure
 254 2b. Furthermore for a given N_e , the genetic correlation and orientation of the \mathbf{G} matrix
 255 become more similar to those of mutation as the strength of selection decreases (increasing
 256 V_s , lighter ellipses in Fig. 1b-e, and rightmost values in Fig. 2b).

257 We have shown above that the type of mutation-selection regime (HoC vs Gaussian) does
 258 not influence genetic correlations in an infinite population (Fig. 2a), but is it also the case

259 in a finite population with substantial genetic drift? For the HoC regime, the expected \mathbf{G} in
 260 an infinite population is proportional to the expectation of $\frac{\boldsymbol{\alpha}\boldsymbol{\alpha}^t}{\boldsymbol{\alpha}^t\mathbf{V}_s^{-1}\boldsymbol{\alpha}}$ over the distribution of
 261 mutation effects $\boldsymbol{\alpha}$ (Zhang and Hill, 2003, eq. 2). In a finite population, accounting for the
 262 reduction in heterozygosity caused by both stabilizing selection and random genetic drift,
 263 this approximation becomes (adapted from Burger et al., 1989, "stochastic house of cards"
 264 regime)

$$\overline{\mathbf{G}} = 4N_e n \mu E \left[\frac{\boldsymbol{\alpha}\boldsymbol{\alpha}^t}{1 + N_e \boldsymbol{\alpha}^t \mathbf{V}_s^{-1} \boldsymbol{\alpha}} \right] = 4n \mu V_s E \left[\frac{\boldsymbol{\alpha}_\rho \boldsymbol{\alpha}_\rho^t}{V_s / (N_e V_\alpha) + \boldsymbol{\alpha}_\rho^t \mathbf{V}_\rho^{-1} \boldsymbol{\alpha}_\rho} \right], \quad (9)$$

265 where $E[\]$ denotes an expectation over the distribution of mutation effects, and $\boldsymbol{\alpha}_\rho = \boldsymbol{\alpha} / \sqrt{V_\alpha}$
 266 are scaled mutation effects, with covariance matrix \mathbf{M}_ρ as per equation (1). Analogously to
 267 equations (7) and (8), the first scalar term in equation (9) equals the equilibrium genetic
 268 variance for a single trait in the HoC regime, while the expectation includes all the parameters
 269 that determine \mathbf{G} matrix shape. Since elements of \mathbf{V}_ρ and \mathbf{M}_ρ scale on the order 1 (and
 270 hence so do $\boldsymbol{\alpha}^t \mathbf{V}_s^{-1} \boldsymbol{\alpha}$ and elements of $\boldsymbol{\alpha}\boldsymbol{\alpha}^t$), the scalar parameter $V_s / (N_e V_\alpha)$ alone determines
 271 whether the \mathbf{G} matrix is more influenced by mutation, selection, or drift. When $V_s \ll N_e V_\alpha$,
 272 drift can be neglected and the \mathbf{G} matrix has the same shape as in the HoC equilibrium; in
 273 particular, the genetic correlation between two traits is given by equation (5), and is thus
 274 the same as in the Gaussian regime. In contrast when $V_s \gg N_e V_\alpha$, drift dominate and the
 275 \mathbf{G} matrix is proportional to \mathbf{M} , with correlation ρ_m .

276 The stochastic house of cards approximation to the genetic correlation (eq. 9) is some-
 277 what less accurate at predicting results from individual-based simulations than our stochastic
 278 Gaussian approximation in the corresponding regime (eq. 9, Fig. 2c, Fig. S2). However, it

279 does capture a similar pattern, where the genetic correlation tends more rapidly towards the
280 mutational correlational with decreasing strength of selection when the effective population
281 size is smaller.

282 In summary, accounting for genetic drift in finite populations, the genetic correlation
283 spans the same range in all mutation regimes, ranging from the mutational correlation ρ_m
284 when drift dominates, to the compromise between mutation and selection in equation (5)
285 when selection dominates. The mutation regime (Gaussian vs HoC) only determines how
286 the realized genetic correlation interpolates between these two limit cases. In particular, the
287 selection strength V_s^{-1} at which genetic correlations transition from being drift-dominated to
288 selection-dominated is multiplied by $(16N_e\mu)^{-1}$ in the Gaussian regime relative to the HoC
289 regime (eqs.(7) and (9)). When $16N_e\mu < 1$, this means that stronger selection is required to
290 overcome the influence of drift when mutations are abundant but with small effects (Gaussian
291 regime) as compared to rare but with larger effects (and vice versa when $16N_e\mu > 1$). But
292 beyond these changes in the quantitative dependence on the strength of selection (which
293 relate to previous findings for a single trait, Hermisson and Wagner, 2004; Bürger, 2000),
294 the qualitative relationship between genetic correlations and the strength of selection given
295 the effective population size remains the same across mutation regimes (Fig. 2b-c).

296 **Shape, orientation, and correlation**

297 Changes in the relative importance of selection versus genetic drift can influence the shape
298 of the \mathbf{G} matrix (determined by its eigenvalues), its orientation (determined by its eigenvec-

299 tors), or both. Any of these effects can translate into changes in genetic correlations, since
300 the latter are only a summary of \mathbf{G} , which depend on both variances and covariances (and
301 on both eigenvectors and eigenvalues). In particular, genetic correlations may change despite
302 little change in orientation, and no rotation of the axes of the \mathbf{G} matrix. This is illustrated
303 in Fig. 3, which focuses on the special case where \mathbf{V} and \mathbf{M} have the same eigenvectors.
304 When this holds, the eigenvectors of \mathbf{G} are identical to those of \mathbf{V} and \mathbf{M} , as demonstrated
305 in the Appendix A2. This means that the \mathbf{G} matrix does not rotate when changing the
306 relative importance of drift versus selection; all that changes are the amounts of variation
307 (eigenvalues) along the different axes (eigenvectors). Nevertheless, the genetic correlation
308 still changes according to eq. (9) in this example. For instance, when one eigenvalues be-
309 comes dominant, the \mathbf{G} matrix becomes increasingly elongated along one of the eigenvectors
310 (Fig. 3a, Fig. S1), which translates into larger values of genetic correlations (Fig. 3b). In the
311 more general case where \mathbf{V} and \mathbf{M} have different eigenvectors, then changing the relative
312 importance of selection vs drift causes both elongation and rotation of \mathbf{G} (changes in shape
313 and orientation), but without necessarily causing larger changes in genetic correlations.

314 Discussion and Conclusion

315 To what extent are genetic correlations between traits shaped by natural selection, or im-
316 posed by mutation? This question, which in essence traces back to the debate between
317 mutationists and selectionists in the early days of genetics (recently revived in the light
318 of molecular evidence, Nei, 2013), has received considerable attention from evolutionary

319 biologists. In particular, evolutionary quantitative genetic theory has made it clear that,
320 when phenotypic (co)variances arise from an equilibrium between mutation and stabilizing
321 selection, then genetic correlations are a compromise between the correlation of pleiotropic
322 mutation effects on traits, and correlational selection favoring combinations of traits (Lande,
323 1980; Lande and Arnold, 1983; Jones et al., 2003; Turelli, 1985). The latter can be related
324 to the orientation and elongation of the fitness landscape relating the traits to fitness (as
325 illustrated in Fig. 1a). However beyond this shape of the fitness landscape, how does the
326 overall strength of selection (size of the ellipses in Fig. 1a) influence genetic correlations be-
327 tween traits? As selection becomes weaker, the fitness peak becomes flatter, with a broader
328 range of phenotypes having equivalent fitness, so does that reduce the influence of selection
329 on genetic correlations? Perhaps surprisingly, the answer is no in an effectively infinite pop-
330 ulation, which in our simulations was already close to holding for a moderate population size
331 of $N_e = 5000$ individuals. Strikingly, the same compromise between mutation and selection
332 effects on genetic correlations holds regardless of the strength of selection, and regardless
333 of whether genetic (co)variances are caused by common mutations of small effect (Gaus-
334 sian regime, Kimura, 1965; Lande, 1980), or rare mutations of large effect (House-of-cards
335 regime, Turelli, 1984, 1985).

336 However, the strength of selection starts to matter as the effective populations size N_e
337 becomes smaller, as random genetic drift plays a larger role. The reasons is that, for a
338 given N_e the strength of selection shifts the balance between drift-dominated and selection-
339 dominated evolutionary dynamics. Since genetic correlations equal mutational correlations

340 ρ_m in the former domain, but a compromise between mutation and selection (eq. (5)) in the
341 latter, overall mutation has a stronger influence on genetic correlations than selection (Fig.
342 2). Previous analyses of \mathbf{G} matrix evolution under mutation and correlational selection in
343 finite populations has mostly focused on the effect of drift on the stability of the \mathbf{G} matrix
344 over evolutionary time (Jones et al., 2003), and largely overlooked the influence of drift on
345 the expected \mathbf{G} . In fact, this influence can be substantial, as shown here; in particular, it
346 determines how the strength of selection affects genetic correlations.

347 Genetic correlations are often described as a constraint on adaptation (Etterson and
348 Shaw, 2001; Agrawal and Stinchcombe, 2009; Connallon and Hall, 2018), but this need not
349 be true, depending on how the orientation of the \mathbf{G} matrix relates to that of directional
350 or fluctuating selection in a changing environment (Gomulkiewicz and Houle, 2009; Chevin,
351 2013; Duputié et al., 2012). In a constant environment as assumed here, the extent to which
352 genetic correlations constrain adaptation depends on how the \mathbf{G} matrix aligns with the
353 matrix of correlational selection, represented in Figure 1a. Our analytical and simulations
354 results show that genetic correlations, and the overall \mathbf{G} matrix shape, differ more from those
355 favored by correlational selection at lower effective population sizes. Since \mathbf{G} becomes more
356 similar to the mutation matrix \mathbf{M} in this case, this could be interpreted as a mutational
357 constraint on evolution (Nei, 2013). However, this alignment with mutation effects occurs
358 because of a prevalence of genetic drift, which is in fact the main constraint on adaptation in
359 this case, also causing temporal fluctuations in the mean phenotype (Lande, 1979) and the
360 \mathbf{G} matrix itself (Jones et al., 2003), and apparent fluctuating selection (Chevin and Haller,

361 2014).

362 Our analytical results for genetic correlations and the \mathbf{G} matrix at mutation-selection-
363 drift balance in the Gaussian regime (eq. (8)) are valid under frequent mutation (Kimura,
364 1965; Lande, 1980; Bürger, 2000), and we accordingly used high mutation rates in the corre-
365 sponding simulations. However, note that the nature of loci is not explicit in this model, but
366 in any case these do not represent single nucleotides or even genes. Rather, they represent
367 large stretches of effectively non-recombining portions of the genome, which may influence
368 the traits by mutation. Since free recombination is also assumed across these loci (consistent
369 with most previous studies), the latter can even be thought of as small chromosomes, for
370 which mutation rates of the order to 10^{-2} seem reasonable. In addition, we also present
371 theoretical and simulation results at much lower mutation rates (House-of-Cards regime),
372 which lead to similar findings. We assumed universal pleiotropy, whereby all loci have the
373 same distribution of mutation effects on all traits. An interesting extension may be to allow
374 for modular mutation effects, or restricted pleiotropy, whereby each locus can only modify
375 a subset of traits by mutations (Chebib and Guillaume, 2017; Chevin et al., 2010), to inves-
376 tigate whether the mutation regime has a stronger effect on mutation correlations in these
377 scenarios. In terms of selection, we considered a fitness peak with an optimum, in line with
378 most theory on the topic, but genetic correlations can also be favored by other forms of se-
379 lection, notably disruptive selection (Bolstad et al., 2015), or negative frequency dependence
380 caused by individual interactions (Mullon and Lehmann, 2019), which may lead to different
381 dependencies of genetic correlations on the strength of selection and genetic drift.

382 Our results lead to some predictions about how genetic correlations should change along
383 lifetime. For traits with ontogenic trajectories, or traits involved in senescence, the pheno-
384 typic value at different ages can be considered as different character states, partly controlled
385 by different loci. This underlies both the mutation accumulation theory of senescence ap-
386 plied to quantitative traits (Charlesworth and Hughes, 1996), and the theory of evolution of
387 growth trajectories (Kirkpatrick and Lofsvold, 1992). If the shape of correlational selection
388 does not change with age, then we only expect a reduced strength of selection in older age,
389 because these ages have a smaller reproductive value and hence contribute less to fitness
390 (Lande, 1982; Charlesworth, 1993). We would then predict that genetic correlations should
391 lean more towards mutational correlations in older ages, but only when the effective popula-
392 tion size is small, while genetic correlations should remain largely unchanged along lifetime
393 in large populations. This pattern can be investigated by measuring genetic correlations
394 among primary traits (not direct components of fitness) across ages, for different species
395 that differ in effective population size (as estimated by e.g. their molecular polymorphism
396 level).

397 More broadly speaking, we expect mutational correlations to impose more constraints on
398 evolutionary trajectories in situations where the population size has been reduced, such as
399 bottlenecks during colonization of novel habitats. Since these situations are also likely to
400 be associated with strong directional selection, this should represent a double challenge for
401 colonizing species. Nevertheless, the extent to which mutational correlations *per se* impede
402 responses to directional selection is unclear. Even when genetic correlations are largely

403 shaped by correlational selection (rather than just by mutation), they may still constrain
404 adaptation, if directional selection in a novel or changing environment does not align with
405 the shape of the fitness peak (Chevin, 2013). In any case, our clear delineation of when, and
406 how much, the strength of selection influences genetic correlations, should provide guidelines
407 for analyzing and interpreting genetic constraints on adaptation in the wild.

408 **Acknowledgments**

409 SC wish to thank Thomas Hansen, David Houle and Christophe Pélabon for discussions on
410 preliminary results. The authors declare no conflicts of interest. This work was supported
411 by the European Research Council (Grant 678140-FluctEvol).

412 **Author Contributions**

413 SC and LMC conceived the study. SC developed analytical solutions for the Gaussian
414 regime. LMC developed analytical solutions for the House-of-Cards regime. SC developed
415 and performed individual-based simulations. SC and LMC wrote the manuscript.

416 **Data Accessibility**

417 The C++ software developed and used to perform genetically explicit individual-based sim-
418 ulations will be available under GPL licence on Github after acceptance.

419 References

- 420 Agrawal, A. F. and Stinchcombe, J. R. (2009). How much do genetic covariances alter the rate
421 of adaptation? *Proceedings of the Royal Society B: Biological Sciences*, 276(1659):1183–
422 1191.
- 423 Bolstad, G. H., Cassara, J. A., Márquez, E., Hansen, T. F., Van Der Linde, K., Houle, D.,
424 and Pélabon, C. (2015). Complex constraints on allometry revealed by artificial selection
425 on the wing of *Drosophila melanogaster*. *Proceedings of the National Academy of Sciences*
426 *of the United States of America*, 112(43):13284–13289.
- 427 Bulmer, M. G. (1989). Maintenance of genetic variability by mutation - selection balance:
428 A child's guide through the jungle. *Genome*, 31(2):761–767.
- 429 Bürger, R. (2000). *The mathematical theory of selection, recombination, and mutation*.
430 Wiley.
- 431 Burger, R., Wagner, G. P., and Stettinger, F. (1989). How Much Heritable Variation Can be
432 Maintained in Finite Populations by Mutation-Selection Balance? *Evolution*, 43(8):1748.
- 433 Charlesworth, B. (1993). Natural selection on multivariate traits in age-structured popula-
434 tions. *Proceedings of the Royal Society B: Biological Sciences*, 251(1330):47–52.
- 435 Charlesworth, B. and Hughes, K. A. (1996). Age-specific inbreeding depression and com-
436 ponents of genetic variance in relation to the evolution of senescence. *Proceedings of the*
437 *National Academy of Sciences of the United States of America*, 93(12):6140–6145.

- 438 Chebib, J. and Guillaume, F. (2017). What affects the predictability of evolutionary con-
439 straints using a G-matrix? The relative effects of modular pleiotropy and mutational
440 correlation. *Evolution*, 71(10):2298–2312.
- 441 Chevin, L. M. (2013). Genetic constraints on adaptation to a changing environment. *Evo-*
442 *lution*, 67(3):708–721.
- 443 Chevin, L. M. and Haller, B. C. (2014). The temporal distribution of directional gradients
444 under selection for an optimum. *Evolution*, 68(12):3381–3394.
- 445 Chevin, L.-M., Martin, G., and Lenormand, T. (2010). Fisher’s Model and the Genomics
446 of Adaptation: Restricted Pleiotropy, Heterogenous Mutation, and Parallel Evolution.
447 *Evolution*, 64(11):3213–3231.
- 448 Connallon, T. and Hall, M. D. (2018). Genetic constraints on adaptation: a theoretical
449 primer for the genomics era. *Annals of the New York Academy of Sciences*, 1422(1):65–87.
- 450 Duputié, A., Massol, F., Chuine, I., Kirkpatrick, M., and Ronce, O. (2012). How do ge-
451 netic correlations affect species range shifts in a changing environment? *Ecology Letters*,
452 15(3):251–259.
- 453 Etterson, J. R. and Shaw, R. G. (2001). Constraint to adaptive evolution in response to
454 global warming. *Science*, 294(5540):151–154.
- 455 Fisher, R. A. (1930). *The genetical theory of natural selection*, volume 154 of *Clarendon*
456 *Press*. Clarendon Press.

- 457 Gomulkiewicz, R. and Houle, D. (2009). Demographic and genetic constraints on evolution.
458 *The American naturalist*, 174(6):E218–29.
- 459 Hansen, T. F. and Houle, D. (2008). Measuring and comparing evolvability and constraint
460 in multivariate characters. *Journal of evolutionary biology*, 21(5):1201–19.
- 461 Hermisson, J. and Wagner, G. P. (2004). The population genetic theory of hidden variation
462 and genetic robustness. *Genetics*, 168(4):2271–2284.
- 463 Houle, D., Bolstad, G. H., Van Der Linde, K., and Hansen, T. F. (2017). Mutation predicts
464 40 million years of fly wing evolution. *Nature*, 548(7668):447–450.
- 465 Hutchinson, G. E. (1957). Concluding Remarks. *Cold Spring Harbor Symposia on Quanti-*
466 *tative Biology*, 22(0):415–427.
- 467 Johnson, T. and Barton, N. (2005). Theoretical models of selection and mutation on quan-
468 titative traits.
- 469 Jones, A. G., Arnold, S. J., and Bürger, R. (2003). Stability of the G-matrix in a popula-
470 tion experiencing pleiotropic mutation, stabilizing selection, and genetic drift. *Evolution*,
471 57(8):1747–1760.
- 472 Jones, A. G., Arnold, S. J., and Bürger, R. (2004). Evolution and stability of the G-matrix
473 on a landscape with a moving optimum. *Evolution*, 58:1639–1654.
- 474 Jones, A. G., Bürger, R., and Arnold, S. J. (2014). Epistasis and natural selection shape the
475 mutational architecture of complex traits. *Nature Communications*, 5:ncomms4709.

- 476 Jones, A. G., Bürger, R., Arnold, S. J., Hohenlohe, P. A., and Uyeda, J. C. (2012). The
477 effects of stochastic and episodic movement of the optimum on the evolution of the G-
478 matrix and the response of the trait mean to selection. *Journal of Evolutionary Biology*,
479 25(11):2210–2231.
- 480 Kimura, M. (1965). A stochastic model concerning the maintenance of genetic variability
481 in quantitative characters. *Proceedings of the National Academy of Sciences of the United*
482 *States of America*, 54(3):731–736.
- 483 Kirkpatrick, M. and Lofsvold, D. (1992). Measuring Selection and Constraint in the Evolu-
484 tion of Growth. *Evolution*, 46(4):954–971.
- 485 Lande, R. (1976). Natural Selection and Random Genetic Drift in Phenotypic Evolution.
486 *Evolution*, 30(2):314–334.
- 487 Lande, R. (1979). Quantitative genetic analysis of multivariate evolution, applied to brain:
488 body size allometry. *Evolution*, 33:402–416.
- 489 Lande, R. (1980). The Genetic Covariance between Characters Maintained by Pleiotropic
490 Mutations. *Genetics*, 94(1):203–15.
- 491 Lande, R. (1982). A Quantitative Genetic Theory of Life History Evolution. *Ecology*,
492 63(3):607–615.
- 493 Lande, R. and Arnold, S. J. (1983). The Measurement of Selection on Correlated Characters.
494 *Evolution*, 37(6):1210–1226.

- 495 Mullon, C. and Lehmann, L. (2019). An evolutionary quantitative genetics model for phe-
496 notypic (co)variances under limited dispersal, with an application to socially synergistic
497 traits. *Evolution*, 73(9):1695–1728.
- 498 Nei, M. (2013). *Mutation-driven evolution*. Oxford University Press.
- 499 Orr, H. A. (2000). Adaptation and the cost of complexity. *Evolution*, 54(1):13–20.
- 500 Revell, L. J. (2007). The G matrix under fluctuating correlational mutation and selection.
501 *Evolution*, 61(8):1857–1872.
- 502 Schluter, D. (1996). Adaptive Radiation Along Genetic Lines of Least Resistance. *Evolution*,
503 50(5):1766–1774.
- 504 Turelli, M. (1984). Heritable genetic variation via mutation-selection balance: Lerch’s zeta
505 meets the abdominal bristle. *Theoretical Population Biology*, 25(2):138–193.
- 506 Turelli, M. (1985). Effects of pleiotropy on predictions concerning mutation-selection balance
507 for polygenic traits. *Genetics*, 111(1):165–195.
- 508 Walsh, B. and Blows, M. W. (2009). Abundant Genetic Variation + Strong Selection =
509 Multivariate Genetic Constraints: A Geometric View of Adaptation. *Annual Review of*
510 *Ecology, Evolution, and Systematics*, 40(1):41–59.
- 511 Zhang, X. S. and Hill, W. G. (2003). Multivariate stabilizing selection and pleiotropy in the
512 maintenance of quantitative genetic variation. *Evolution*, 57(8):1761–1775.

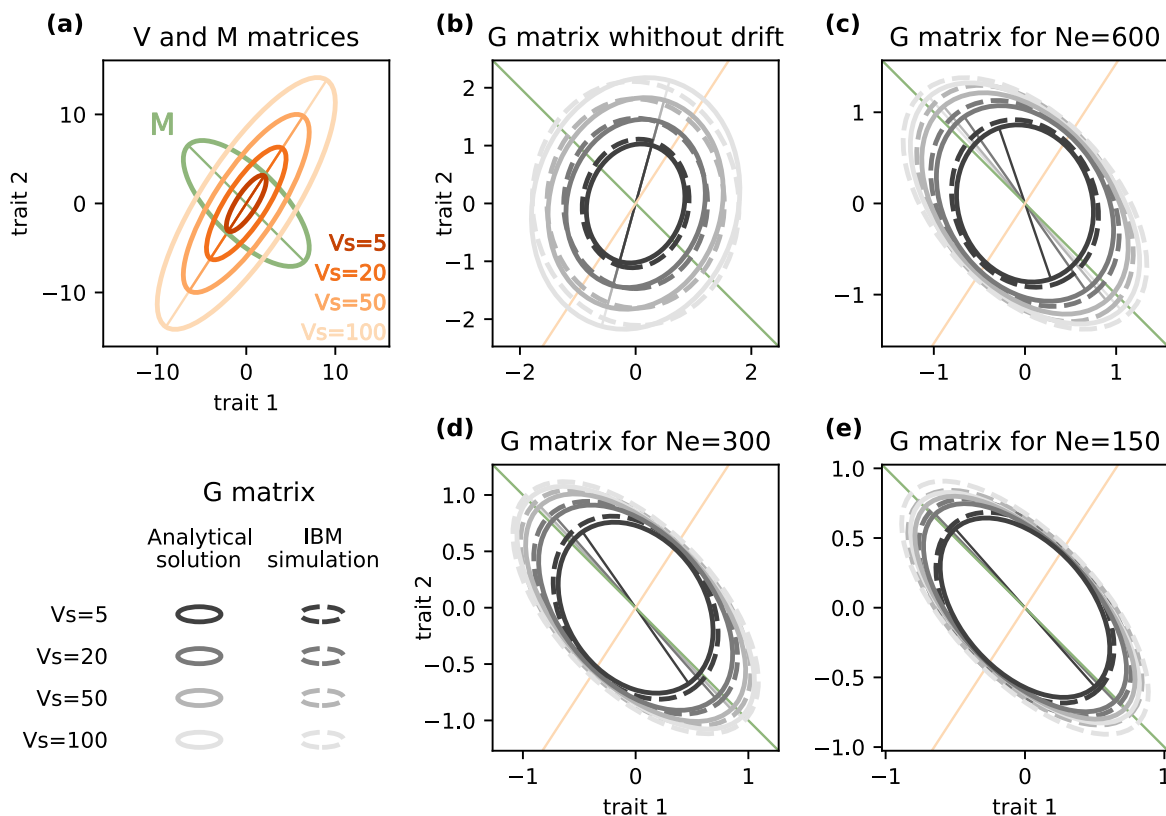


Figure 1: **Influence of selection strength and genetic drift on the G matrix (Gaussian regime).** (a) Orientation and shape of the mutation matrix M , and selection matrix V with variable selection strengths. First eigenvectors are represented with colored lines. (b-e) Shape and orientation of the G matrix as the width of the fitness peak V_s varies. Solid ellipses (along with their first eigenvectors) represent the analytical predictions from equation (7) that neglects genetic drift in (b), or equation (8) that accounts for genetic drift in (c-e). Dashed ellipses show the mean estimates from IBM simulations with $N_e = 5000$ (b), 600 (c), 300 (d) and 150 (e). Parameters used: $n = 50$, $\mu = 0.01$, $\rho_m = -0.7$, $\phi_m = 1$, $V_\alpha = 0.0025$ and $\rho_s = 0.8$, $\phi_s = 2$, and $V_s = 5, 20, 50, 100$.

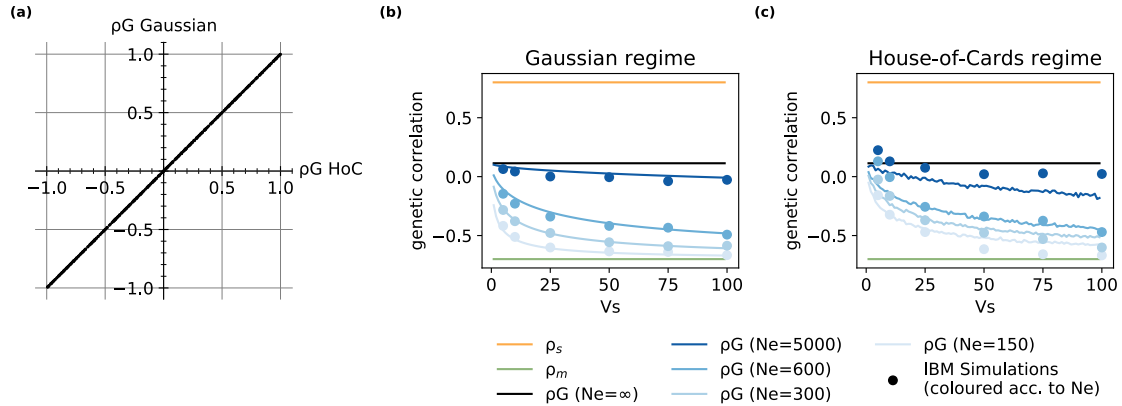


Figure 2: Influence of selection strength and genetic drift on genetic correlations under different mutation regimes (a) The genetic correlation in an infinite population, at equilibrium between selection and abundant mutations of weak effects (Gaussian approximation, from eq. (7)) is plotted against its expectation under rare mutations of large effects (house-of-cards approximation, eq. 5), for 500 random pairs of mutation \mathbf{M} and selection \mathbf{V} matrices. (b-c) The genetic correlation is plotted against the width of the fitness peak V_s , for different effective sizes N_e . The parameters values in (b) are the same as in Figure 1, corresponding to the Gaussian mutation regime. In (c), the mutation parameters are instead $V_\alpha = 0.05$ and $\mu = 0.0002$, corresponding to the House-of-cards regime. Blue points correspond to the genetic correlation simulated with individual-based models (IBM). The black line represents the analytical expectation without drift (eq. (5)) in both cases. The blue lines represent the analytical prediction with drift (eq. (8)) in (b), and expectations over 10000 randomly drawn mutation effects α (from eq. (9)) in (c).

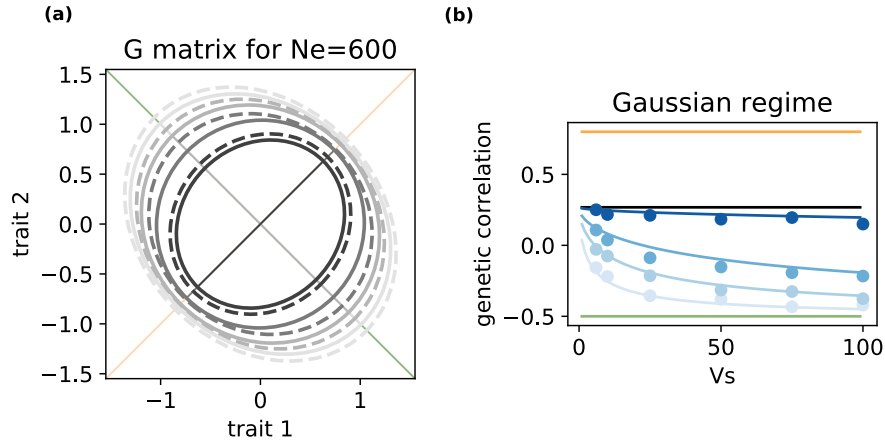


Figure 3: **Influence of selection strength and genetic drift on genetic correlations in the special case where \mathbf{V} and \mathbf{M} have the same eigenvectors.** (a) Shape and orientation of the \mathbf{G} matrix as the width of the fitness peak V_s varies. In this illustrative example where $N_e = 600$, the first eigenvector of the \mathbf{G} matrix (plain lines, from gray to black) is orientated either fully along the major axis for selection (eigenvector of \mathbf{V} , orange line) or for mutation (eigenvector of \mathbf{M} , green line), depending on the selection parameter V_s . (b) The genetic correlation is plotted against the width of the fitness peak V_s , for different effective sizes N_e as in Figure 2. Note that, although axes of the \mathbf{G} matrix do not rotate, the influence of selection strength and genetic drift on genetic correlations is comparable to the general case in Figure 2. Parameters are identical to Figure 1, except that $\phi_s = \phi_m = 1$ such that \mathbf{V} and \mathbf{M} have the same eigenvectors, $\rho_m = -0.5$, and the strongest selection is for $V_s = 6$ instead of 5.

513 **A Appendix: How does the strength of selection influ-** 514 **ence genetic correlations ?**

515 **A.1 Steps for solving the mutation-selection-drift equilibrium**

By building on the Gaussian approximation of the continuum-of-allele model (Kimura, 1965) and assuming infinite-sized population with non-overlapping generations, Lande (1980) derived a simple expression for genetic covariance matrix equilibrium (\mathbf{G}) selection-mutation balance. We here extend this result to allow for random genetic drift. At equilibrium, the production of genetic variance due to new polygenic mutations is balanced by the loss of genetic variance to due both stabilizing selection and random drift (Lande, 1979). For a single haploid locus we obtain :

$$\mu\mathbf{M} = \overline{\mathbf{G}}\mathbf{V}^{-1}\overline{\mathbf{G}} + \frac{1}{2N_e}\overline{\mathbf{G}}$$

516 where $\overline{\mathbf{G}}$ denotes an expectation over the stochastic evolutionary process (because of random
517 genetic drift).

Introducing $\mathbf{B} = \frac{1}{2N_e}\mathbf{I}$ and $\mathbf{U} = \mu\mathbf{M}$, this becomes

$$\mathbf{U} = \overline{\mathbf{G}}\mathbf{V}^{-1}\overline{\mathbf{G}} + \mathbf{B}\mathbf{G}$$

$$\mathbf{V}^{-\frac{1}{2}}\mathbf{U}\mathbf{V}^{-\frac{1}{2}} = \mathbf{V}^{-\frac{1}{2}}\overline{\mathbf{G}}\mathbf{V}^{-\frac{1}{2}}\mathbf{V}^{-\frac{1}{2}}\overline{\mathbf{G}}\mathbf{V}^{-\frac{1}{2}} + \mathbf{V}^{-\frac{1}{2}}\mathbf{B}\mathbf{G}\mathbf{V}^{-\frac{1}{2}}$$

By defining $\mathbf{V}^{-\frac{1}{2}}\overline{\mathbf{G}}\mathbf{V}^{-\frac{1}{2}} = \mathbf{X}$ and $\mathbf{V}^{-\frac{1}{2}}\mathbf{U}\mathbf{V}^{-\frac{1}{2}} = -\mathbf{C}$, we finally have to solve the quadratic matrix equation :

$$\mathbf{0} = \mathbf{X}^2 + \mathbf{B}\mathbf{X} + \mathbf{C}$$

A quadratic matrix equation can be solved explicitly if the following requirements are met:

(i) \mathbf{X}^2 is preceded by an identity matrix, (ii) \mathbf{B} commutes with \mathbf{C} , and (iii) $\mathbf{B}^2 - 4\mathbf{C}$ has a square root. The solution of the quadratic matrix equation is then :

$$\mathbf{X} = -\frac{1}{2}\mathbf{B} + \frac{1}{2}(\mathbf{B}^2 - 4\mathbf{C})^{\frac{1}{2}}$$

In our case, an explicit solution for \mathbf{X} exists. Indeed, \mathbf{X}^2 is preceded by an identity matrix, \mathbf{B} is a diagonal matrix and then always commute with \mathbf{C} . Finally, as \mathbf{B}^2 and \mathbf{C} are both positive semi-definite then $(\mathbf{B}^2 - 4\mathbf{C})^{1/2}$ will always have a solution. Recall that

$$\mathbf{V}^{-\frac{1}{2}}\overline{\mathbf{G}}\mathbf{V}^{-\frac{1}{2}} = \mathbf{X}$$

then

$$\begin{aligned}\overline{\mathbf{G}} &= \mathbf{V}^{\frac{1}{2}}\mathbf{X}\mathbf{V}^{\frac{1}{2}} \\ \overline{\mathbf{G}} &= \mathbf{V}^{\frac{1}{2}} \left[-\frac{1}{2}\mathbf{B} + \frac{1}{2}(\mathbf{B}^2 - 4\mathbf{C})^{\frac{1}{2}} \right] \mathbf{V}^{\frac{1}{2}} \\ \overline{\mathbf{G}} &= \mathbf{V}^{\frac{1}{2}} \left[-\frac{1}{4Ne}\mathbf{I} + \frac{1}{2} \left(\frac{1}{(2Ne)^2}\mathbf{I}^2 + 4\mathbf{V}^{-\frac{1}{2}}\mathbf{U}\mathbf{V}^{-\frac{1}{2}} \right)^{\frac{1}{2}} \right] \mathbf{V}^{\frac{1}{2}}\end{aligned}$$

518 Finally by using notations (1) and (4), we obtain equation (8)

519 **A.2 Constraints on the orientation and shape of the \mathbf{G} matrix**
 520 **in the special cases where \mathbf{V} and \mathbf{M} matrices have the same**
 521 **eigenvectors**

522 **A.2.1 Case without drift**

523 Starting from equation (7)

$$\mathbf{G} = 2n\sqrt{\mu V_\alpha V_s} \mathbf{V}_\rho^{\frac{1}{2}} \left[\mathbf{V}_\rho^{-\frac{1}{2}} \mathbf{M}_\rho \mathbf{V}_\rho^{-\frac{1}{2}} \right]^{\frac{1}{2}} \mathbf{V}_\rho^{\frac{1}{2}}$$

524 and assuming that both matrices \mathbf{V}_ρ and \mathbf{M}_ρ have the same eigenvectors \mathbf{Q} but different
 525 eigenvalues, their spectral decompositions give $\mathbf{V}_\rho = \mathbf{Q}\mathbf{\Lambda}_s\mathbf{Q}^{-1}$ and $\mathbf{M}_\rho = \mathbf{Q}\mathbf{\Lambda}_m\mathbf{Q}^{-1}$ respec-
 526 tively, where $\mathbf{\Lambda}_w$ and $\mathbf{\Lambda}_m$ are diagonal matrices of eigenvalues. Then, equation (7) can be
 527 simplified to

$$\mathbf{G} = 2n\sqrt{\mu V_\alpha V_s} \mathbf{Q} [\mathbf{\Lambda}_w \mathbf{\Lambda}_m]^{\frac{1}{2}} \mathbf{Q}^{-1}$$

528 This shows that \mathbf{G} matrix has the same eigenvectors \mathbf{Q} as the \mathbf{V} and \mathbf{M} matrices, and that
 529 its eigenvalues are the geometric means of eigenvalues of \mathbf{V} and \mathbf{M} .

530 **A.2.2 Case with drift**

531 Starting from equation (8)

$$\overline{\mathbf{G}} = 2n\sqrt{\mu V_\alpha V_s} \mathbf{V}_\rho^{\frac{1}{2}} \left[\left(\frac{V_s}{(4N_e)^2 \mu V_\alpha} \mathbf{I}^2 + \mathbf{V}_\rho^{-\frac{1}{2}} \mathbf{M}_\rho \mathbf{V}_\rho^{-\frac{1}{2}} \right)^{\frac{1}{2}} - \sqrt{\frac{V_s}{(4N_e)^2 \mu V_\alpha}} \mathbf{I} \right] \mathbf{V}_\rho^{\frac{1}{2}}$$

532 and performing a spectral decomposition of \mathbf{V}_ρ and \mathbf{M}_ρ as in the case without drift (see
 533 above), after simplification we obtain :

$$\bar{\mathbf{G}} = 2n\sqrt{\mu V_\alpha V_s} \mathbf{Q} \left[\left[\frac{V_s}{(4N_e)^2 \mu V_\alpha} \mathbf{\Lambda}_s^2 + \mathbf{\Lambda}_s \mathbf{\Lambda}_m \right]^{\frac{1}{2}} - \frac{V_s}{(4N_e)^2 \mu V_\alpha} \mathbf{\Lambda}_s \right] \mathbf{Q}^{-1}$$

534 While the eigenvalues of \mathbf{G} are given by the equation located between the highest level of
535 brackets, the eigenvectors of \mathbf{G} still equal \mathbf{Q} the same as \mathbf{V} and \mathbf{M} matrices.

536 **A.2.3 Graphical representation of G matrix in the special case where V and M**
 537 **matrices have the same eigenvectors**

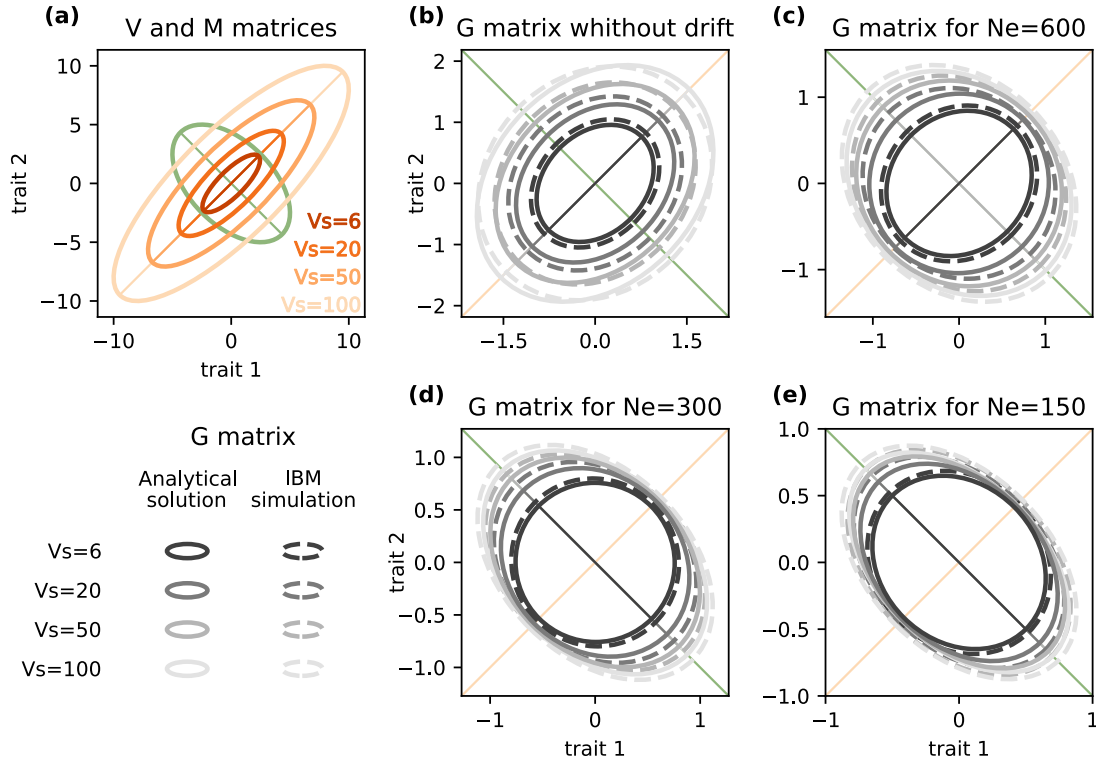


Figure S1: **Influence of selection strength and genetic drift on the G matrix when V and M matrices have the same eigenvectors.** (a) Orientation and shape of M and V matrices for respectively $\rho_m = -0.5$, $\phi_m = 1$, $V_\alpha = 0.05$, $\rho_s = 0.7$, $\phi_s = 1$, $V_\alpha = 6, 20, 50, 100$. (b-f) see Figure 1 for a detailed legend.

538 **A.3 G matrix in the House of cards regime**

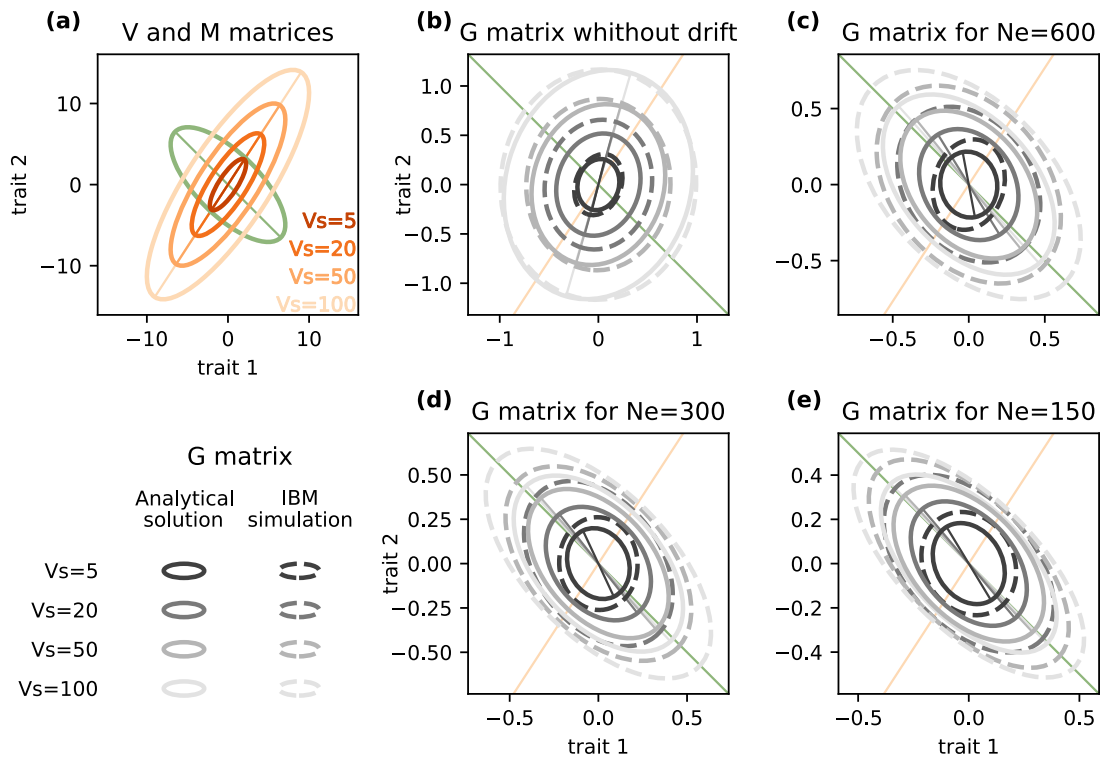


Figure S2: **Influence of selection strength and genetic drift on the G matrix (House-of-Cards regime)**. (a) Orientation and shape of **M** and **V** matrices for respectively $\rho_m = -0.7$, $\phi_m = 1$, $V_\alpha = 0.05$ and $\rho_s = 0.8$, $\phi_s = 2$, $V_s = 5, 10, 50, 100$. First eigenvectors are represented colored lines. We set $n=50$ and the $\mu = 0.0002$. (b-f) see Figure 1 for a detailed legend.